ESOMAT 2009, 05003 (2009)
DOI:10.1051/esomat/200905003
© Owned by the authors, published by EDP Sciences, 2009

Comparative study of the structures of Fe-Mn-Si-Cr-Ni shape memory alloys obtained by classical and by powder metallurgy, respectively

L. G. Bujoreanu [a1] , S. Stanciu[1], B. Özkal[2], R. I. Comăneci[1], M. Meyer[3]

[1] Faculty of Materials Science and Engineering, The "Gh. Asachi" Technical University from Iaşi, Bd. D. Mangeron 61A, 700050 Iaşi. Romania
[2] Particulate Materials Laboratory, Metallurgical and Materials Engineering Department, Istanbul Technical University, 34469 Maslak – Istanbul, Turkey
[3] NETZSCH Gerätebau GmbH, Wittelsbacherstrasse 42, Selb/ Bavaria, 95100, Germany

Abstract. Hot rolled specimens of low-manganese Fe-Mn-Si-Cr-Ni shape memory alloys, produced by classical and by powder metallurgy (CM and PM) with mechanical alloying, respectively, were analysed by tensile loading-unloading tests (TENS), by dilatometry (DIL), by X-ray diffraction (XRD) and scanning electron microscopy (SEM). Solution annealed specimens had two-phase structure, comprising γ-austenite and thermally induced α-martensite. The formation of α'-stress-induced martensite during TENS was ascertained by SEM and XRD being accompanied by rounded loading portions on stress-strain curves, characteristic to transformation induced plasticity, which preceded long stress plateaus with low tilt. Even if loading behaviour changed from transformation induced plasticity, on first loading, to slip induced plasticity, during subsequent ones, the specimens maintained their pseudoelastic behaviour on each unloading. DIL responses of the elongated CM and PM specimens emphasised a thermally-induced reversion, noticeable only during first heating, which was associated with thermally induced reversion of α-stress-induced martensite.

1. Introduction

Fe-Mn-Si based shape memory alloys (SMAs), were discovered as single crystals by Sato *et al* [1], were developed as polycrystals by Murakami *et al.* based on Fe-30 Mn-6 Si (mass. %, as all compositions will be listed hereinafter) [2], gained corrosion resistance as an effect of Cr and Ni additions performed by Otsuka *et al.* and finally became potential candidates for low price (as compared to NiTi base alloys) SMA applications, under the form of: Fe-28 Mn-6 Si-5 Cr [3] and Fe-14 Mn-5 Si-9 Cr-5 Ni [4].

Since Fe-Mn-Si based SMAs experience a γ (face centre cubic, fcc) ↔ ε (hexagonal close packed, hcp) martensitic transformation, shape memory effect (SME) relays to the obtainment of ε stress induced martensite on deformation and on its thermally induced reversion on heating [5]. Considering its crucial role in SME-occurrence, the stress-induced formation of ε (hcp) martensite has been intensely studied [6-9] and its reversion to γ (fcc) has been examined as an effect of thermal actuation on heating [10-14] or as an effect of simple mechanical unloading [15-17] or even by going further, to compression, in such a way that a mechanism for reversible plasticity was proposed based on the sequence $\varepsilon_{tensile} \leftrightarrow \gamma \leftrightarrow \varepsilon_{compression}$ [18].

At low Mn content or at high deformation degrees, α' (body centre cubic, bcc) ferromagnetic martensite is stress induced [19] the presence of which is undesirable from the point of view of transformation reversibility [20]. It is noticeable that α' (bcc) martensite can be thermally induced in low-Mn Fe base alloys [21] or can be stress-induced from ε martensite [22] its formation being ascribed to an intersecting shear mechanism of ε plate variants [23]. Essentially, it was reported that α' martensite formed in two steps, γ → ε → α', is different from that directly formed from austenite, γ → α', since the former is stress (strain) induced while the latter is thermally induced [24] under the form of lenticular plates [25]. Nevertheless, it is generally accepted that in Fe-Mn-Si based SMAs α' martensite doesn't revert to austenite on heating, regardless it is thermally or stress induced.

[a] e-mail: lgbujor@tuiasi.ro

This is an Open Access article distributed under the terms of the Creative Commons Attribution-Noncommercial License (http://creativecommons.org/licenses/by-nc/3.0/), which permits unrestricted use, distribution, and reproduction in any noncommercial medium, provided the original work is properly cited.

Article available at http://www.esomat.org or http://dx.doi.org/10.1051/esomat/200905003

Most of the reports on Fe-Mn-Si based SMAs refer to specimens produced by classical metallurgy (CM), comprising ingot obtainment by means of melting, alloying and casting, while only scarce reports refer to alternative manufacturing technologies such as rapid solidification [26]. The general opinion is that Fe-Mn-Si based SMAs are useful as long as their manufacturing costs, including the price of metallic components and the costs of technological processing, are less than those of Ni-Ti based SMAs. However, CM processing involves several drawbacks, such as Si incorporation into melt, manganese loss on melting, chemical composition homogenization, cooling contraction of ingots and during quenching, etc., which render technological flow rather complicated [27]. For this reason the present paper aims to introduce powder metallurgy (PM) as alternative manufacturing technology for Fe-Mn-Si based SMAs-obtainment, and to compare the results with those obtained by CM. It is noticeable that, as far as the knowledge of authors goes, such a comparative study was not reported yet in literature.

2. Experimental procedure

An Fe-18Mn-3Si-7Cr-4Ni SMA was produced by classical metallurgy (CM) and by powder metallurgy (PM). CM manufacturing technology involved high frequency induction melting under Ar atmosphere and casting into a cylindrical mould with inner diameter of 8×10^{-3} m. PM manufacturing involved pressing and sintering at 1390 K, under cracked ammonia (75 % N_2 + 25 % H_2), of mechanically alloyed (MA) commercial powders, with zinc stearate binder. In order to decrease thickness down to about 1×10^{-3} m and to increase compactness, homogenization annealing, (1370K/ 1 hr. /water) and hot rolling, 1270 K were applied both to CM and PM specimens. The above mentioned chemical composition was confirmed by spectrogravimetry, the amount of carbon being determined as 0.06 C. This composition meets the alloy design criteria given by eq. (6) in [28], which require that the composition of an alloy must be located in γ-phase zone of the Schaeffler phase diagram.

Both CM and PM specimens were analyzed by tensile loading-unloading tests (TENS), by dilatometry (DIL), by X-ray diffraction (XRD) and by scanning electron microscopy (SEM). TENS were performed on an INSTRON 3382 tensile testing machine with a deformation rate of 2.77×10^{-4} sec^{-1}. Dilatometry was carried out on a NETZSCH DIL 402 CD dilatometer, at a heating rate of 8.33 x 10^{-2} K/s up to 870 K, under He atmosphere, using fused silica and alumina as sample holder material and standard calibration material, respectively. XRD observations were done on a BRUKER AXS D8 Advance diffractometer with Cu K_α SEM analysis was conducted on a SEM – VEGA II LSH TESCAN scanning electron microscope, coupled with an EDX – QUANTAX QX2 ROENTEC detector.

3. Experimental results and discussion

3.1 Mechanical response

Two representative tensile stress-strain curves for CM specimens are illustrated in Fig. 1.

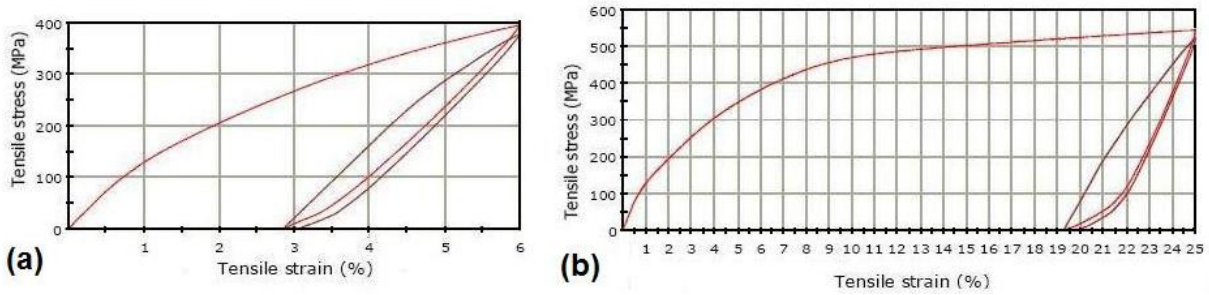

Fig.1 Stress-strain curves recorded during tensile loading-unloading tests of Fe-18Mn-3Si-7Cr-4Ni (mass. %) SMA obtained by CM: (a) up to 6 % total strain, during two cycles; (b) up to 25 % total strain, during two cycles

As compared to typical slip induced plasticity of plain carbon steels, with Hookian initial region, the deformation illustrated in Fig. 1 reveals plastic regions which are more rounded, being characterized by higher work hardening rate. This deformation behaviour, which misses the well defined stress plateaus noticeable in β-type SMAs [29], is characteristic for transformation induced plasticity (TRIP) [30].

However TRIP occurred only during first loading which suggests that, for CM specimens, stress induced martensitic transformation is the governing deformation mechanism only during first loading while slip becomes prominent during subsequent loadings. On the other hand, in both cases illustrated in Fig. 1 unloading is accompanied by additional spring back which is the main of characteristic pseudoelasticity [31], being obvious even after 25 % straining, in Fig. 1(b). Regardless loading behaviour, unloading behaviour remained unchanged,

and pseudoelasticity is noticeable during subsequent cycles, even after applied strains as high as 25 %. After cutting their fastening ends, tensile CM specimens, subjected to total strains of 4; 8 and 12 %, were analysed by dilatometry, while other set of specimens subjected to total strains of 4; 5 and 6 % were analysed by XRD.

TRIP-characteristic deformation behaviour during first loading is also noticeable in the case of PM specimens as shown in the representative tensile stress-strain curves illustrated in Fig. 2.

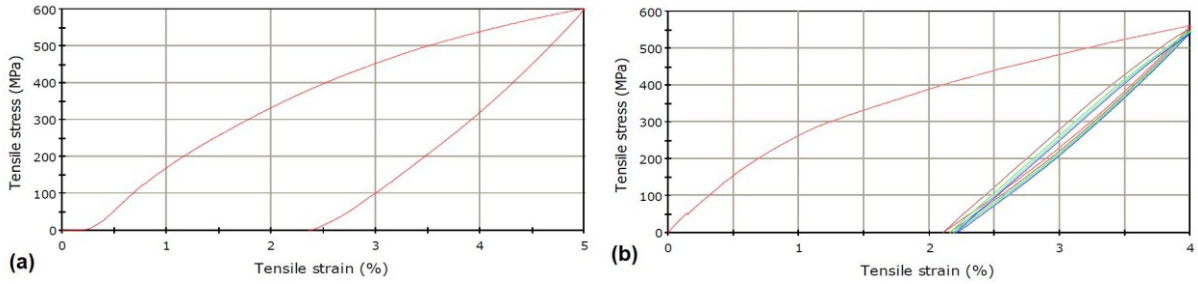

Fig.2 Stress-strain curves recorded during tensile loading-unloading tests of Fe-18Mn-3Si-7Cr-4Ni (mass. %) SMA obtained by PM: (a) up to 5 % total strain; (b) up to 4 % total strain, during five cycles

As in the case of CM specimens, PM specimens revealed TRIP behaviour only during first loading while slip-induced plasticity behaviour became obvious during subsequent loadings, as in Fig. 2(b). As compared to CM specimens, PM specimens revealed much less pseudoelastic character but appeared to be tougher. This could be an effect of mechanical alloying (MA) which, in the case of low-Mn Fe based alloys, enhances deformation hardening due to the formation of brittle α' martensite [32]. After cutting their fastening ends, the specimens elongated with 4; 5 and 5.6 % were analysed by dilatometry and XRD.

3.2 Thermal response

Dilatometry enabled accurate monitoring of relative elongation (dL/L_0) and of thermal expansion coefficient (α) during temperature variation on heating. Both for CM and PM specimens, solid state transitions were accompanied by local decreases of α, as shown in Fig.3.

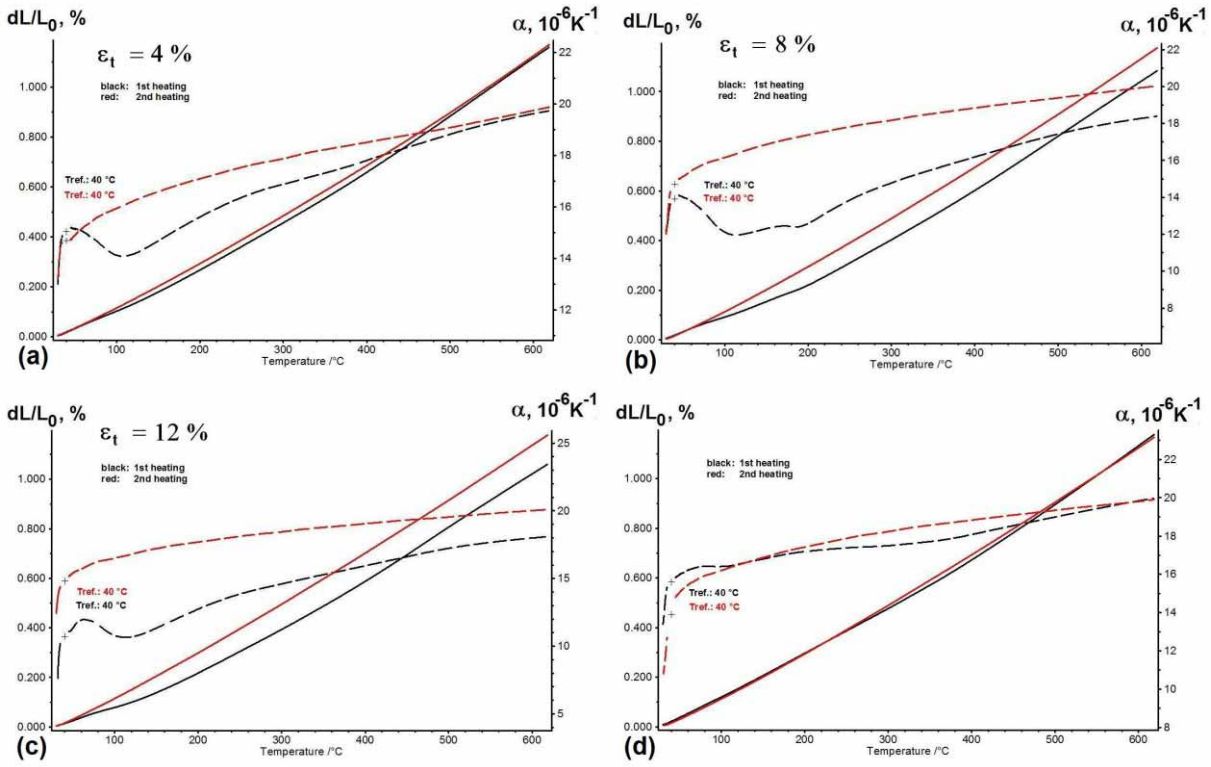

Fig. 3 Variations with temperature of relative elongation (dL/L_0, with solid line) and of thermal expansion coefficient (α, with dashed line), on the dilatograms recorded during the heating of strained specimens of Fe-18Mn-3Si-7Cr-4Ni (mass. %) SMA: (a) CM specimen pre-strained with 4 %; (b) CM specimen pre-strained with 8 %; (c) CM specimen pre-strained with 12 %; (d) PM specimen pre-strained with 5 %;

Both CM and PM specimens revealed more prominent thermally induced transformations during the first heating as compared to second heating, the difference being more obvious in the variation of α coefficient. The transitions became more prominent with increasing maximum applied strain, from 4 to 8 and finally to 12 %, as noticeable from Fig. 3(a) to (b) and (c), respectively. By comparing α variation with temperature of CM and PM specimen, Fig. 3(d), it is obvious that the transition has been less prominent in the latter.

A better insight on the solid state transition occurring in elongated specimens during first heating is obtained in Fig. 4, by comparing the variation of relative elongation (dL/ L_0) with temperature of the three CM specimens elongated with 4; 8 and 12 %, respectively and that of a PM specimen elongated with 5 %.

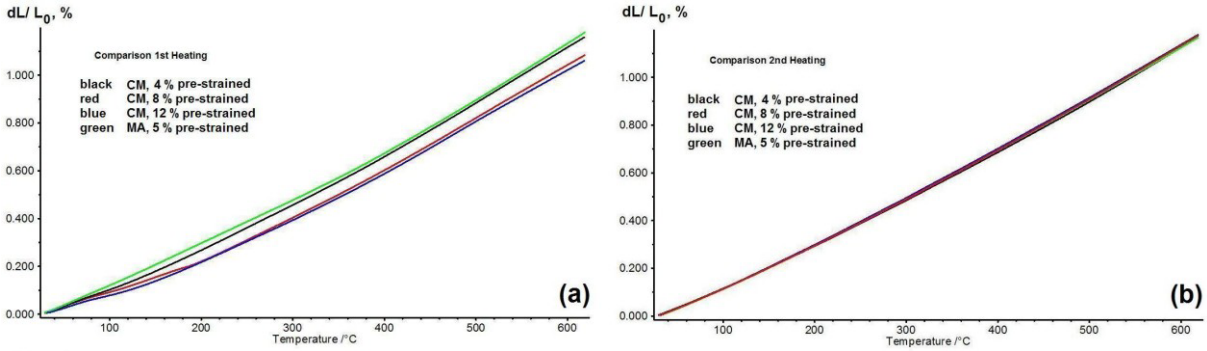

Fig. 4 Comparison of the thermal responses of Fe-18Mn-3Si-7Cr-4Ni SMA specimens, obtained by CM and by PM with MA, illustrating the variation with temperature of relative elongation: (a) during first heating; (b) during second heating

It is obvious that the transition has been enhanced by increasing maximum applied strain but had the lowest intensity in the case of the PM specimen, Fig. 4(a). On the other hand, Fig. 4(b) shows that the same comparison performed during the second heating revealed that the differences between CM and PM specimens and between differently elongated CM specimens became negligible.

This observation ascertains the assumption that a solid state transition occurred only in pre-strained specimens, during first heating, being enhanced by the increase of applied strain and being more obvious at CM than at PM specimens.

3.3 Structural analysis

The XRD patterns of CM specimens, shown in Fig. 5, revealed the presence of only four diffraction maxima.

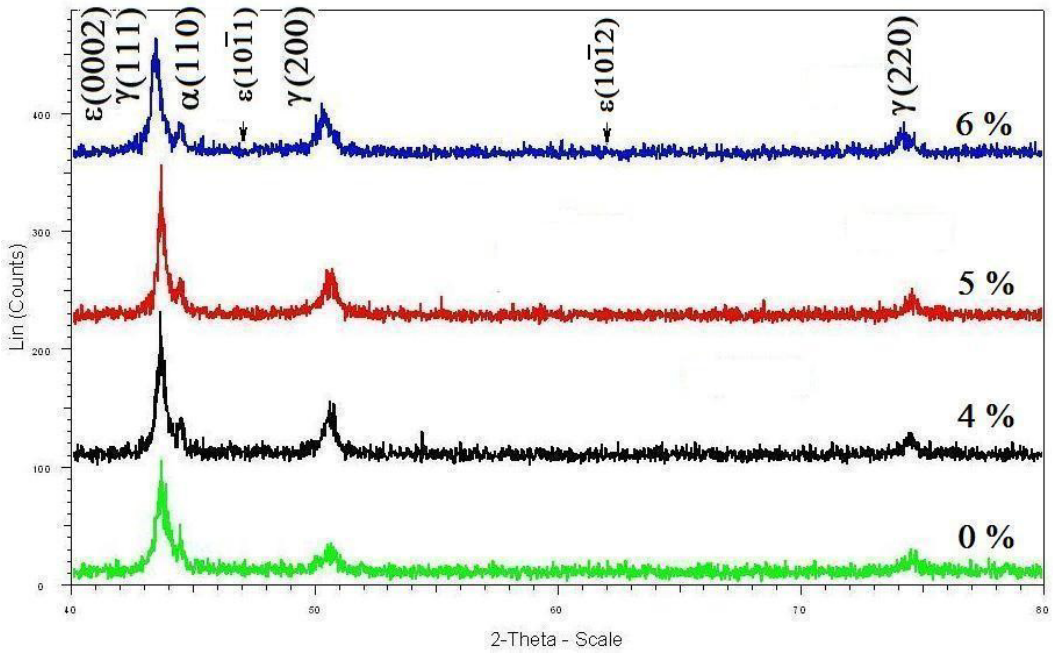

Fig. 5 XRD patterns recorded on the gauges of tensile CM specimens of Fe-18Mn-3Si-7Cr-4Ni (mass. %) SMA, after being subjected to tensile loading-unloading tests, up to various maximum strains

In accordance to phase indexing performed by means of EVA software, the most probable phase correspondent of the peaks are γ(111)/ ε(0002); α(110); γ(200) and γ(220), respectively. The quantitative analysis, displayed in Table 1 ascertained the augmenting tendency of *d* interplanar spacings with increasing maximum applied strain.

Table 1. Quantitative analysis of XRD patterns shown in Fig. 5, corresponding to CM specimens

Maximum strain, %	0		4		5		6	
	d, nm	%	d, nm	%	d, nm	%	d, nm	%
$\gamma_{(111)}$ $\varepsilon_{(0002)}$	0.207224	60.2	0.207208	53.5	0.207063	55.3	0.208096	53.8
$\alpha_{(110)}$	0.203519	5.1	0.20354	7.2	0.203687	4.5	0.203562	5.6
$\gamma_{(200)}$	0.18032	24.5	0.180244	27.5	0.18029	32.1	0.180867	27.5
$\gamma_{(220)}$	0.127256	10.2	0.127287	11.8	0.127114	8.1	0.127596	13.1

The spacings listed for $\alpha_{(110)}$, ranging between 0.203519 and 0.0203687 nm, are close enough to the value found in literature, $d_{\alpha(110)}$ = 0.02026 nm [33]. For all of the phases *d* had larger values at 6 % strain than at 0 % strain. The general tendency of the amount of α phase was to increase with maximum applied strain.

The XRD patterns of PM specimens revealed the same main four diffraction maxima ascribed to the same metallographic phases: γ(111)/ ε(0002); α(110); γ(200) and γ(220) as noticeable from the smoothened diagrams shown in Fig. 6. The results of corresponding quantitative analysis are listed in Table 2.

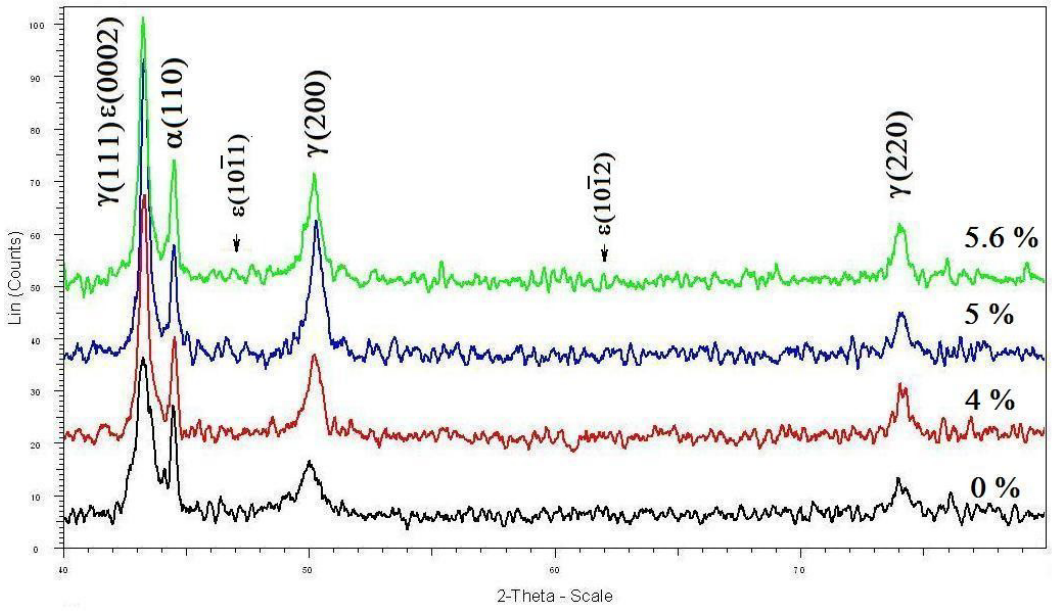

Fig.6 Smoothened XRD patterns recorded on the gauges of tensile PM specimens of Fe-18Mn-3Si-7Cr-4Ni (mass. %) SMA after being subjected to tensile loading-unloading tests, up to various maximum strains

Table 2. Quantitative analysis of XRD patterns shown in Fig. 6, corresponding to PM specimens

Maximum strain, %	0		4		5		5.6	
	d, nm	%	d, nm	%	d, nm	%	d, nm	%
$\gamma_{(111)}$ $\varepsilon_{(0002)}$	0.20928	56.3	0.209002	49.5	0.20893	49.5	0.20911	44.8
$\alpha_{(110)}$	0.203577	12	0.203519	11.3	0.203219	10.7	0.203745	13
$\gamma_{(200)}$	0.181994	17.8	0.18184	25.3	0.181308	28	0.181716	28.2
$\gamma_{(220)}$	0.127746	13.9	0.127719	13.9	0.127827	11.8	0.127847	14

When comparing the results for CM and PM specimens, it seems that not all of the metallographic phases present in PM specimens had larger *d* values at 5.6 % strain than at 0 % strain. It is noticeable that the amount of α phase has been at least double, as compared to CM specimens, but revealed the same general tendency to increase with increasing the applied strain.

Summarizing the results obtained by XRD it appears that no ε thermally or stress induced martensite has been identified, yet α' martensite was readily observed, owing to its $\alpha_{(110)}$ main diffraction peak [34]. This means that the solid state transition observed by dilatometry would simply correspond to the reversion to austenite of α' stress induced martensite, on heating, since there is no other martensitic phase in both CM and PM alloys. The fact that the transition occurred only during first heating, of pre-strained specimens sustains this assumption. However the presence of martensite has to be further confirmed.

Four representative SEM micrographs recorded on CM and PM specimens in unstrained and strained states are shown in Fig. 7.

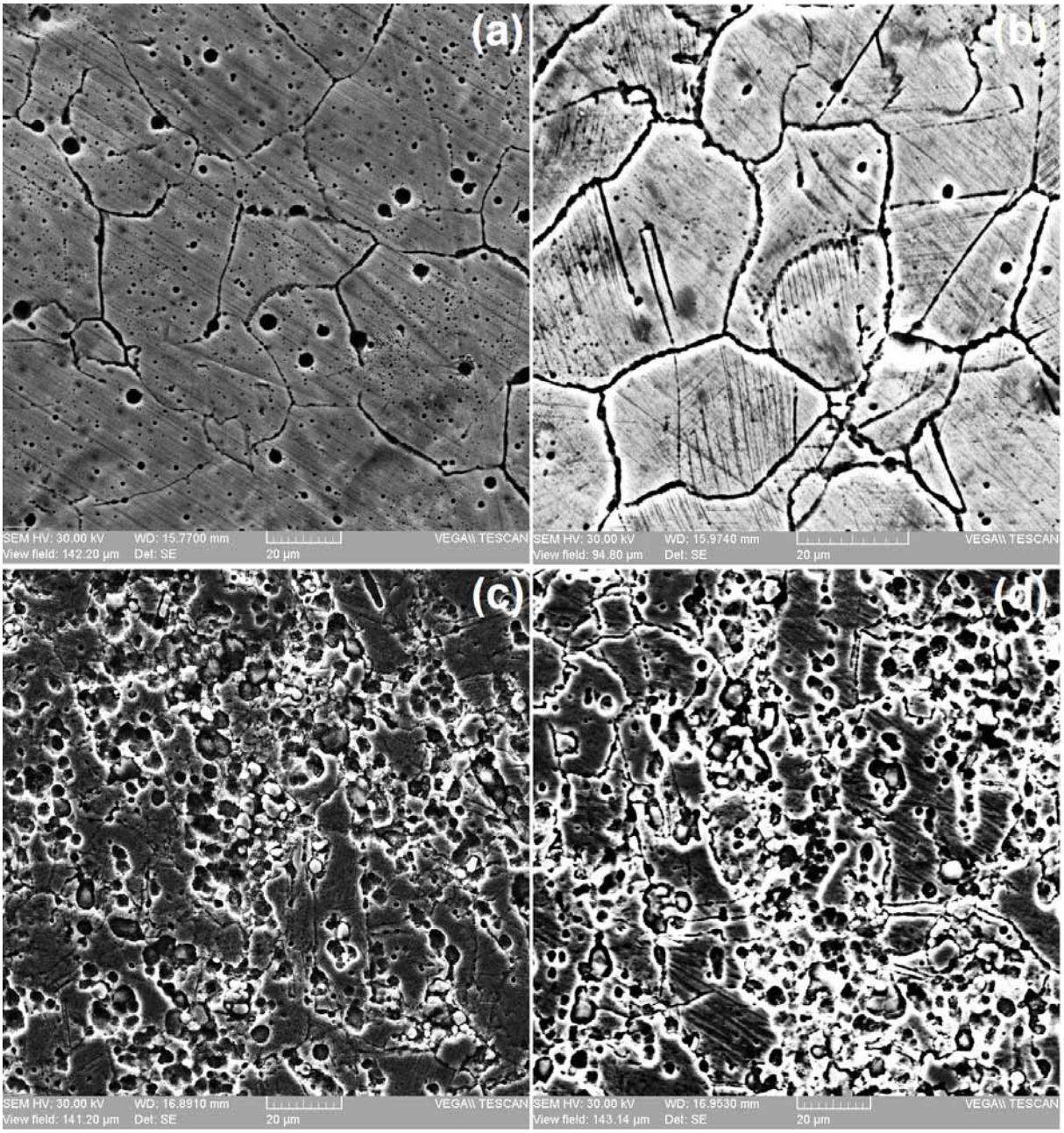

Fig. 7 SEM micrographs illustrating the structure of Fe-18Mn-3Si-7Cr-4Ni (mass. %) SMA: (a) CM specimen in unstrained state; (b) CM specimen pre-strained with 6 %; (c) PM specimen in unstrained state; (d) PM specimen pre-strained with 5 %

No α' thermally induced martensite is noticeable on the micrograph of CM unstrained specimen in Fig. 7(a), in spite of its approx. 5 % proportion displayed in Table 1. However, the micrograph of PM unstrained

specimen, Fig. 7(c), reveals scarce α' thermally induced martensite plates with dark contrast [35], since this phase would represent an amount of 12 %, in accordance to Table 2.

Recently Maji et al. reported that, in a Fe-14 Mn-6 Si-9 Cr-5 Ni SMA, the formation of α' bcc martensite was favoured by the increase of the amount of thickness-reduction by cold rolling, which induced a strong texture effect and that α' martensite formation was also favoured by the application of an annealing heat treatment after cold rolling. All their conclusions sustained the formation of α' martensite not directly from γ austenite but from ε, as an effect of the interaction of martensite plate variant [36].

However though the alloy under study, with the nominal composition Fe-18 Mn-3 Si-7 Cr-4 Ni, respects alloy design criteria given in [28], it enables the formation of α' thermally induced martensite directly from γ austenite as an effect of homogenization annealing. Moreover, dilatometric observations revealed that α'stress induced martensite reverts to austenite during first heating.

4. Summary and conclusions

Both CM and PM specimens of Fe-18Mn-3Si-7Cr-4Ni alloy revealed transformation-induced plasticity during the first tensile loading and slip induced plasticity during subsequent ones and pseudoelasticity, characterized by additional spring backs present even after 25 % straining, during unloading. The pseudoelastic character was more prominent at CM specimens as compared to PM specimens yet the latter experienced higher stress levels, which were associated with larger amounts of α' thermally induced martensite. On the other hand, CM specimens were more ductile since they experienced strains as high as 25 % while all PM specimens failed at strains above 6 %. Therefore, from the point of view of mechanical response it seems that CM and PM specimens behave similarly yet the former are more ductile and pseudoelastic while the latter are tougher due to larger amounts of α'martensite.

Both CM and PM pre-strained specimens experienced a solid state transition during first heating, which was absent during second heating. Considering that α' martensite was the single martensitic phase identified in the alloy's microstructure, both by XRD and SEM, it is assumed that this transition could be ascribed to thermally-induced reversion to austenite of α'stress-induced martensite, on heating.

Since no distinctive ε-corresponding peaks were noticed on the XRD patterns of the pre-strained specimens, it can be assumed that the main stress induced martensite would be α' and not ε. The amount of α'martensite increased with increasing the applied strain, both in CM and PM specimens, and its presence was ascertained by XRD and SEM.

The present results are the first report on PM-manufactured Fe-Mn-Si-Cr-Ni alloys experiencing a thermally induced reversion of stress induced martensite. However, additional work is necessary in order to check the occurrence of shape memory effect as an effect of training.

Acknowledgements This work was financially supported by UEFISCU by means of the research grant PN II-ID 301-PCE-2007-1, contract no. 279/01.10.2007.

Special thanks are brought to Dr. Takahiro Sawaguchi and his co-workers, Dr. Takehiko Kikuchi, Dr. Kazuyuki Ogawa and Mr. Motomichi Koyama, from NIMS, Tsukuba, for scientific guidance and support.

References

[1] A. Sato, E. Chishima, K. Soma, T. Mori, Acta metall. **30**, 1177 **(**1982)

[2] M. Murakami, H. Otsuka, H.G. Suzuki, S. Matsuda, "Complete shape memory effect in polycrystalline Fe-Mn-Si alloys" Proc. Int. Conf. on Martensitic Transformation, Nara, Japan, 1986, (The Japan Institute of Metals, 1986), p. 985

[3] H. Otsuka, H. Yamada, T. Maruyama, H.; Tanahashi, S.; Matsuda, M. Murakami, ISIJ Int, **30** 674 (1990)

[4] Y. Moriya, H. Kimura, S. Ishizaki, S. Hashizume, S. Suzuki, H. Suzuki and T. Sampei, J Phys **III**, Vol. 1, novembre C4-433 (1991)

[5] T. Maki, "Ferrous shape memory alloys", Shape Memory Materials, edited K. Otsuka and C.M. Wayman, (Cambridge, University Press, 1998), p. 133

[6] A.P. Gulyaev, T.F. Volynova, Metal Sci Heat Treat. **21(2),** 98 (1979)

[7] Y. Tomota, M. Strum, J.W. Morris, Metall. Mater. Trans. A, **19(6)**, 1563, (1988)

[8] T. Kikuchi, S. Kajiwara, Y. Tomota, Mater Trans **36(6**), 719, (1995)

[9] T.Y.Hsu, Science in China E, **40(6)**, 561 (1997)

[10] M. Murakami, H. Otsuka, H.G. Suzuki, S. Matsuda, Trans ISIJ **27** B88 (1987)

[11] M. Sade, K. Halter, E. Hornbogen, “Transformation behaviour and one-way shape memory effect in Fe-Mn-Si alloys”, Progress in Shape Memory Alloys, edited by S. Eucken, (DGM-Informationsgesellschaft Verlag, Bochum, 1992), p 191
[12] M. Sade, K. Halter, E. Hornbogen, “The effect of thermal cycling on the transformation behaviour of Fe-Mn-Si shape memory alloys”, Progress in Shape Memory Alloys, edited by S. Eucken, (DGM-Informationsgesellschaft Verlag, Bochum, 1992), p 201
[13] Y. Tomota, T. Maki, Mater. Sci Forum **327-328** 191 (2000)
[14] J. Tang, Mater. Sci Forum **327-328** 239 (2000)
[15] O. Matsumura, T. Sumi, N. Tamura, K. Sakao, T. Furukawa, H, Otsuka, Mater. Sci. Eng. A **279** 201 (2000)
[16] T. Sawaguchi, T. Kikuchi, S. Kajiwara, Smart Mater. Struct. **14** S317 (2005)
[17] Y.H. Wen, W.L. Xie, N. Li, D. Li, Mater. Sci. Eng. A **457** 334 (2007)
[18] T. Sawaguchi, L.G. Bujoreanu, T. Kikuchi, K. Ogawa, M. Koyama, M. Murakami, Scripta Mater **59** 826 (2008)
[19] L. Bracke, G. Mertens, J. Penning, B.C. De Cooman, M. Liebeherr, N. Akdut, Metall. Mater. Trans. A, **37A**, February, 307 (2006)
[20] B. Dubois, Trait. Thermique, **234**, 27 (1990)
[21] Y. Tomota, M. Strum, J.W. Morris Jr., Metall. Trans. A, **18 June**, 1073, (1987)
[22] Y. Tomota, M. Strum, J.W. Morris Jr., Metall. Trans. A, **17 March**, 537, (1986)
[23] J.H. Yang, C.M.Wayman, Metall Trans A **23 May** 1445 (1992)
[24] B.X. Huang, X.D. Wang, Y.H. Rong, L. Wang, L. Jin, Mater Sci Eng A **438–440** 306 (2006)
[25] B.C. Maji, M. Krishnan, V.V. Rama Rao, Metall Mater Trans A **34 May**, 1029 (2003)
[26] P. Donner, , M. Sade, E. Hornbogen, “Shape memory effect in meltspun Fe-Mn-Si shape memory alloys”, Progress in Shape Memory Alloys, edited by S. Eucken, (DGM-Informationsgesellschaft Verlag, Bochum, 1992), p 289
[27] A.K. Sinha, *Ferrous Physical Metallurgy*, (Butterworth, Boston, 1989). pp. 14-17; 327-369
[28] J.C. Li, M. Zhao, Q. Jiang, , Metall Mater Trans A **31 March**, 581 (2000)
[29] N. Stanford, D.P. Dunne, Mater Sci Eng A **422** 352 (2006)
[30] N. Gu, C. Lin, X. Song, H. Peng, F. Yin, Q. Liu, Mater. Sci Forum **327-328** 231 (2000)
[31] T.W. Duerig, R. Zadno, „An engineer’s perspective of pseudoelasticity", Engineering Aspects of Shape Memory Alloys, edited by T.W. Duerig, K.N. Melton, D. Stöckel, C.M. Wayman, (Butterworth-Heinemann, New York, 1990), p. 369
[32] V. V. Cherdyntsev, L. Yu. Pustov, S. D. Kaloshkin, I. A. Tomilin, E. V. Shelekhov, A. I. Laptev, Yu. V. Baldokhin, E. I. Estrin, Fizika Metallov i Metallovedenie, **104(4)** 423 (2007)
[33] S. S. M. Tavares, A. Lafuente, S. Miraglia, D. Fruchart, J mater Sci **37** 1645 (2002)
[34] K.M. Mostafa, J. De Baerdemaeker, N. Van Caenegem, D. Segers, and Y. Houbaert, J Mater Perform doi 10.1007/s11665-009-9474-y (2009)
[35] S.-H. Lee, H.-J. Kim, J.-H. Jun, S.-H. Baik, C.-S. Choi, Mater. Sci Forum **327-328** 227 (2000)
[36] B.C. Maji, M. Krishnan, V. Hiwarkar, I. Samajdar, R.K. Ray, J Mater Perform doi 10.1007/s11665-009-9428-4 (2009)